ISIJ International, Vol. 44 (2004), No. 10, pp. 1774–1779

Thermodynamic Analysis on the Dust Generation from EAF for the Recycling of Dust

Yoshiaki KASHIWAYA, Akira TSUBONE,[1)] Kuniyoshi ISHII and Hirohiko SASAMOTO

Graduate School of Engineering, Hokkaido University, Sapporo 060-8628 Japan. E-mail: Yoshiaki@eng.hokudai.ac.jp
1) Production Engineering Div., Aichi Steel Co., Japan.

(*Received on March 12, 2004; accepted in final form on July 20, 2004*)

Recently, in addition to the large interest on the CO_2 emission problem, the energy saving and the environmental conservation become more and more important issue. Zero emission campaign is adopted by many companies. In such circumstances, most of steel companies were carrying out the recycling of dust by many ways. There are many aspects on the dust recycling. One of important purpose is the zinc recovery, and other is the utilization as a slag (*e.g.* roadbed material) by injection. Especially for the dust injection, many troubles such as an accumulation in the filtering system and an increase of the content of harmful elements in the dust will occur. Then, it become very important to understand the mechanism and the thermodynamics of the dust generation or/and precipitation form EAF to prevent those troubles.

In this study, the dust sampled from the impeller of blower in the dust filtering system of EAF was examined by XRD and XRF. Quite complicated compounds formed in Zn–Fe–Pb–Cr–Mn–O–Cl–F system were found in the dust according to the dust injection. Thermodynamic analysis was performed and the equilibrium composition obtained from the calculation was in excellent agreement with the actual composition in the dust. Main constituents in the dust are $ZnFe_2O_4$ and Fe_2O_3. Relatively dominant ones are as follows: Fluorides are FeF_3, ZnF_2 and PbF_2, chlorides are $ZnCl_2$ and $PbCl_2$, and oxides are ZnO and MnO_2. The fluorides deposit around 1 000°C from gas phase. And the chlorides ZCl_2, $PbCl_2$ and oxides MnO_2 form less than 500°C. The partial pressure of chloride gas will become a maximum around 400°C, when there is no moisture.

KEY WORDS: dust; thermodynamic analysis; injection of dust; EAF; chlorides; fluorides; zinc recovery.

1. Introduction

As the dust generated in the ironmaking and steelmaking process includes valuable metals such as zinc, lead and iron, it is an important and secondary resource for industrial society. General purpose of the dust processing from metal industry might be the recovery of zinc. While some of company is carrying out the utilization of EAF (electric arc furnace) slag for the material of a roadbed and so on. In such a case, it would be better to utilize the dust as a slag by injecting into the EAF. In the course of dust recycling, as the zinc content in the dust will increase, the added-value of the final dust can increase. However, because of high zinc content in the dust, the reducibility of iron oxide is relatively low. Furthermore, the existence of lead, chlorine and alkali compounds is disturbing the recovery of pure zinc and/or the processing of the dross. Thus, many problems will exist in the recycling of the dust. Moreover, the harmful elements such as the lead, cadmium, hexavalent chromium and fluorine should be utilized by overcoming the environmental problems.

Recently, in addition to the large interest on the CO_2 emission problem, the energy saving and the environmental conservation become more and more important issue. Zero emission campaign is adopted by many companies. The dust processing will be one of an effective way for zero emission. In such circumstances, most of steel companies were carying out the recycling of dust with many ways.[1–7)] Especially, some of the steel companies having EAF carried out the dust injection as the recycle of dust in the plant.[8–15)] It would be very important to understand the mechanism and the thermodynamics of the dust generation form EAF to prevent its accumulation in the filtering system.

A few review exists on the dust recycling in EAF.[16,17)] Thermodynamic analysis on a Zn–Fe–O system was performed by Nakamura *et al.*[18)] According to dust recycling, the contents of zinc, chlorine and fluorine may increase and many troubles such as a deposition of dust inside the filtering system will occur. The system of components becomes more and more complicate and difficult to understand the constituents in the dust.

In this study, XRD (X-ray diffraction) and XRF (X-ray fluorescent) analysis of the deposited dust in the filtering system were carried out and the determination of the compounds in the dust was performed. To understand the mechanism of the dust deposition, thermodynamic analysis for complicated system (Zn–Fe–Pb–Cr–Mn–O–Cl–F) was carried out.

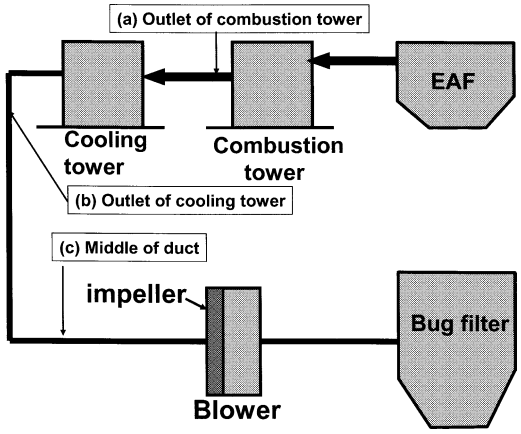

Fig. 1. Flow of dust suction system in EAF (electric arc furnace). (a), (b) and (c) mean the position of sampling, measuring temperature and gas composition.

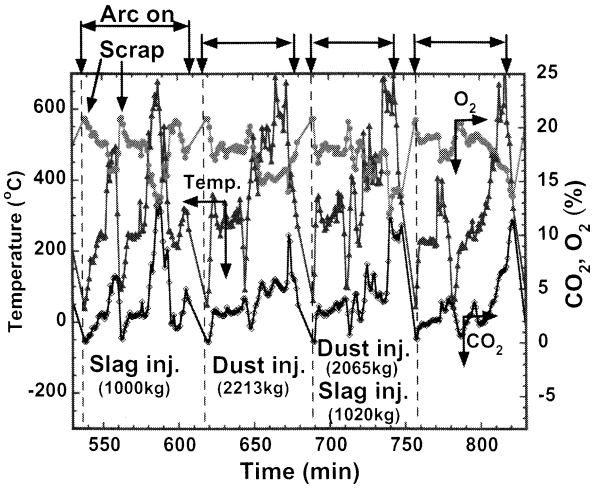

Fig. 2. Variation of O_2%, CO_2% and temperature at the outlet of combustion tower in the dust filtering system.

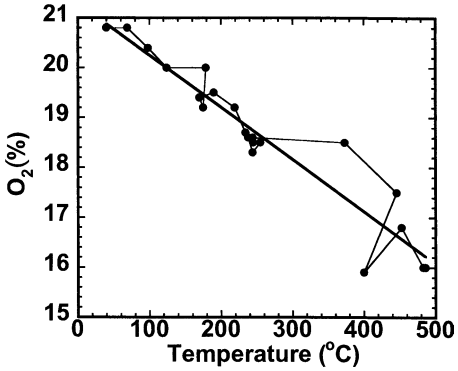

Fig. 3. Relationship between oxygen concentration and temperature at the outlet of combustion tower in the dust filtering system.

2. Facility of Dust Filtering System and Measurement of Temperature and Gas Concentration during Operation

Figure 1 shows the dust filtering system equipped with No. 3 EAF in Aichi Steel Co. The steel pipe with 200 cm in diameter is connected from EAF to the bug filter, in which the combustion tower and the cooling tower are equipped for oxidizing and cooling the generated dust, respectively. The blower having impeller is used for the suction of air including the dust, which flowrate was about 5 600 m^3/min (at 250°C).

Measurements of the temperature and the gas composition of O_2, CO and CO_2 were carried out during operation. Three positions, (a), (b) and (c) were selected for the measurements as shown in Fig. 1. An air is just mixed at the combustion tower for oxidizing the generated dust, because the gas temperature including the dust is high, the oxidation of the dust will proceed easily. The dust temperature gradually decreased from the cooling tower until the blower. The temperature at the position (c) in Fig. 1 was around 200°C (variation was from 100 to 400°C). At the position (a), the temperature was around 500°C and the variation of temperature during the operation accompanied with the dust injection is shown in **Fig. 2**. The variation of O_2 and CO_2 concentration are also shown in Fig. 2. The variation of CO gas was also measured together with O_2 and CO_2. Since the concentration range of CO gas was ppm order and the way of changing was the same as CO_2, CO was neglected from the Fig. 2. Four operations were carried out within 5 h and two scrap charges were performed in each operation. The combination of the dust injection and the slag injection were selected and performed in the respective operation on the basis of the experimental design theory.

The temperature at the outlet of the combustion tower decreased from 500 to 100°C, when the scrap was charged. According to this action, O_2 concentration increased from 15 to 21% and CO_2 decreased from 8 to almost 0%. When the arc was applied, the temperature increased until 500°C rapidly, and the variation of O_2 and CO_2 showed opposite behavior. These behaviors would be resulted from the combustion reaction of carbon and the oxidation reaction of metallic elements evaporated from EAF. The cycle of these variations of temperature and the gas concentrations was almost the same and repeated according to the arc melting operation.

Figure 3 shows the relationship between the concentration of oxygen and the temperature at the position (a). These results will be caused by the following reactions.

$$C + O_2(g) = CO_2(g) \quad \text{.....(1)}$$

$$n\text{Me} + \frac{m}{2} O_2(g) = \text{Me}_n\text{O}_m \quad (\text{Me: metallic element}) \quad \text{.....(2)}$$

The CO_2 increase showed in Fig. 2 would be caused by the reaction (1). If there were no halogen elements (chlorine and fluorine), it is considered that most of compounds in the dust will be an oxide. However, the content of chlorine and fluorine is increasing with the dust recycle operation. **Figure 4** shows the variation of zinc, chlorine and fluorine in the dust during the dust injection operation, in which total dust injection was about 150 tons for the first 10 d. The content of zinc in the dust increased from 24 to 35% and the chlorine increased from 3.8 to 5.3%. During 5 d recess, the zinc and chlorine contents decreased in this period. The behavior of fluorine content was not so clear to the dust injection, however, overall behavior of the fluorine content followed the dust injection.

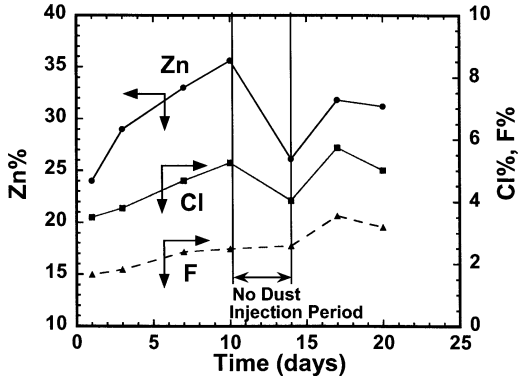

Fig. 4. Variations of Zn, Cl and F in the dust during the dust injection operation.

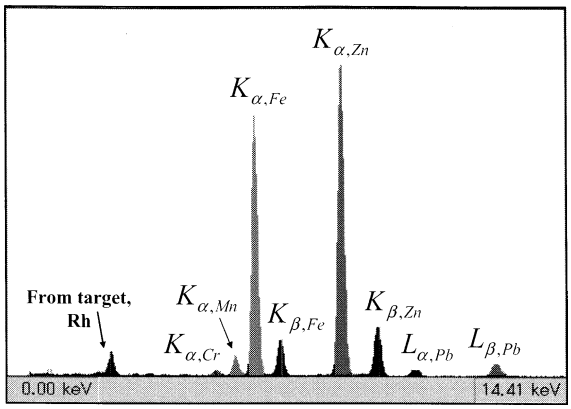

Fig. 5. Result of XRF analysis of the dust.

3. Dust Composition and Distribution of the Elements in the Dust Layer Adhered on the Impeller

Figure 5 shows the result of XRF (X-ray fluorescent) analysis of the dust deposited on the impeller of blower. The main components were zinc and iron, and lead, chrome and manganese were also contained in the dust. Distribution of these elements in the deposited dust layer was measured using μ-XRF (beam size: 100 μm) and showed in **Fig. 6**. The thickness of the layer was about 1 mm. The distribution of each elements consisted of a layer which was roughly parallel to the macroscopic layer. The locations of zinc and iron were almost the same and lead was concentrated in the area where the iron content was low.

This dust layer was crushed and the powder was served to the XRD (X-ray diffraction) analysis for determining the kind of compounds. **Figure 7** shows the result of XRD analysis (the number beside the compound means the one in the ASTM card). It was found that quite complicated compounds existed in the dust. However, almost 100% peaks could be explained. The iron compounds were $ZnFe_2O_4$, Fe_2O_3 and FeF_3, the zinc compounds were ZnO, ZnF_2 and $ZnCl_2$, lead ones were $PbCl_2$, PbF_2 and manganese one was MnO_2. The chromium compound was very small and difficult to detect by XRD.

4. Thermodynamic Analysis of Dust Generation: Zn–Fe–Pb–Mn–Cr–O–Cl–F System

The precise thermodynamic analysis will be difficult for

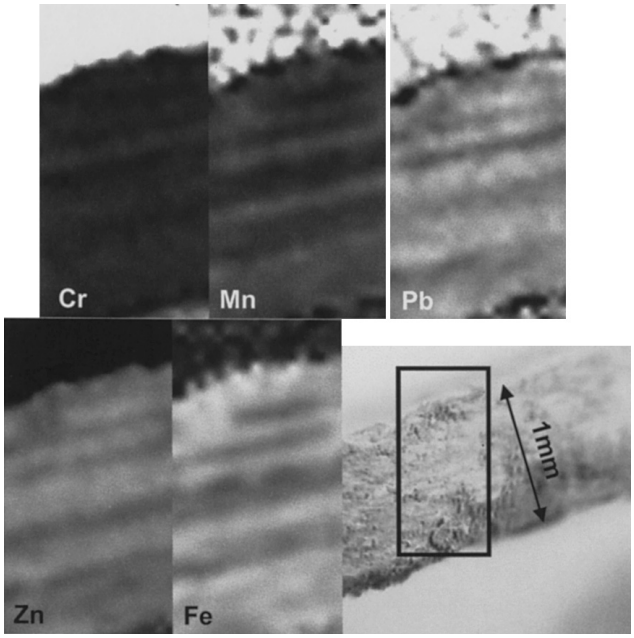

Fig. 6. Distribution of the elements in the dust layer deposited on the impeller (XRF analysis).

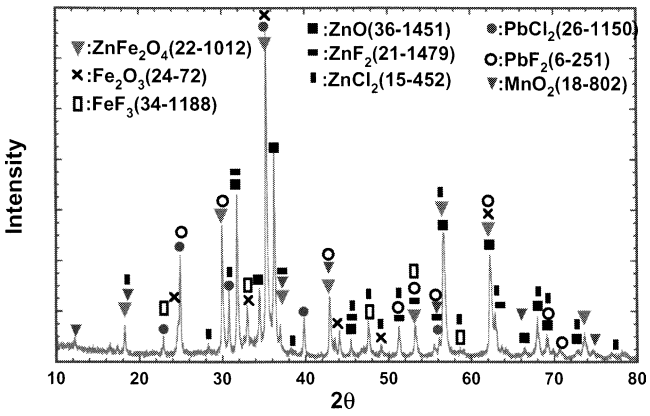

Fig. 7. Result of XRD analysis of the dust deposited on the impeller.

the Zn–Fe–Pb–Mn–Cr–O–Cl–F system. However, as the basic system is Zn–Fe–O–Cl–F system, the preliminary analysis was carried out for Zn–O–Cl–F and Fe–O–Cl–F systems, respectively.

Figure 8 shows the predominance diagrams on the Zn–O–Cl, Zn–O–F and Zn–Cl–F systems. The result of XRD showed the existence of ZnO, ZnF_2 and $ZnCl_2$ (Fig. 7). The possible partial pressure range for the existence of those compounds was examined. As it was considered that the temperature range of the dust deposition would be less than 500°C, the range from 500 to 100°C would be enough temperature range to analyze. In Zn–Cl–F system, both of ZnF_2 and $ZnCl_2$ can be formed in the following range of P_{Cl_2} (Fig. 8(b)).

$$-15 < \log P_{Cl_2} < 0 \quad \text{.....(3)}$$

$$\log P_{F_2} \approx -40 \quad \text{.....(4)}$$

Although the chlorine partial pressure is as high as 1 atm around 150°C, ZnF_2 can be formed, when the partial pressure of F_2 is as low as 1×10^{-40} atm. From Figs. 8(c) and

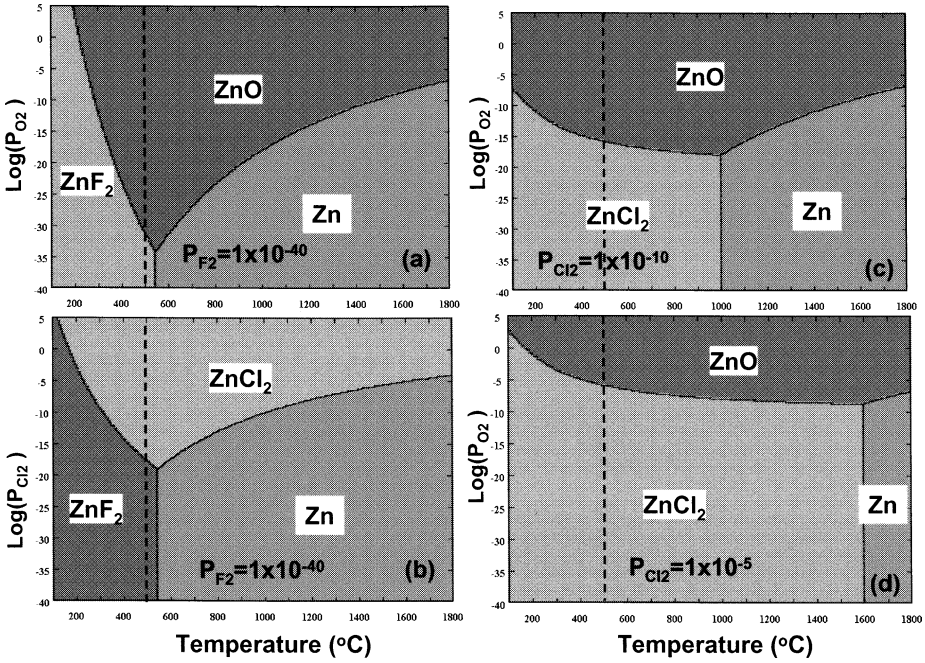

Fig. 8. Predominance diagrams. (a) Zn–F–Cl system ($P_{F_2}=1\times10^{-40}$), (b) Zn–Cl–F system ($P_{F_2}=1\times10^{-40}$), (c) Zn–Cl–O system ($P_{Cl_2}=1\times10^{-10}$) and (d) Zn–Cl–O system ($P_{Cl_2}=1\times10^{-5}$).

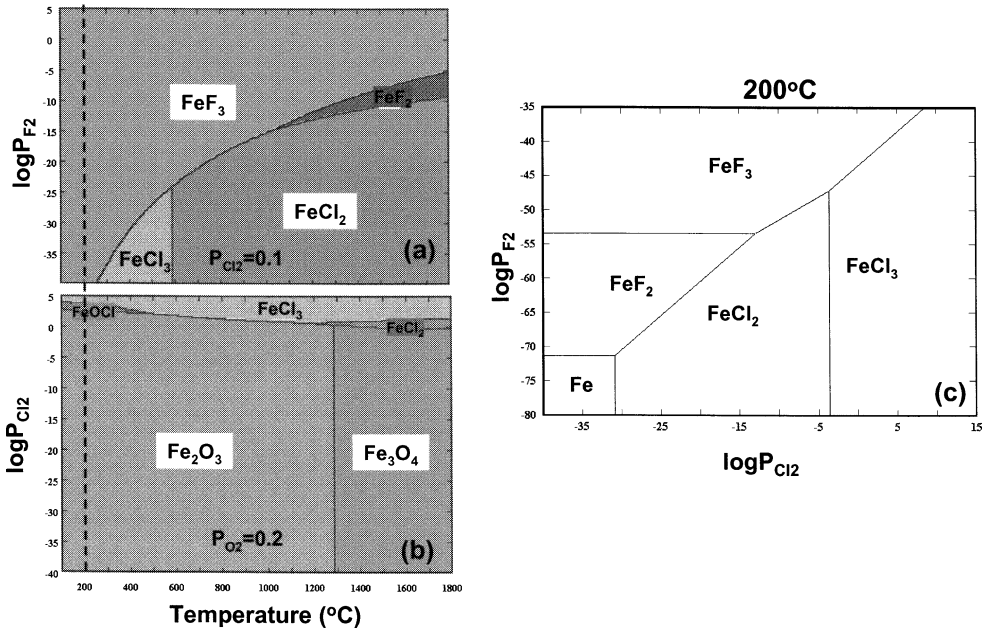

Fig. 9. Predominance diagrams. (a) Fe–F–Cl system ($P_{Cl_2}=0.1$), (b) Fe–Cl–O ($P_{O_2}=0.2$) system and (c) Fe–Cl–F system at 200°C.

8(d), it can be assumed that the partial pressure of chlorine P_{Cl_2} was from 0.001 to 0.0001 atm ($P_{O_2}=0.2$ atm at 500°C), because the P_{Cl_2} should be larger than 1×10^{-5} atm for the coexisting of ZnO and $ZnCl_2$. From these considerations, it was found that the ZnF_2 would be always dominant when there was small quantity of fluorine existing in the system. And the partial pressure of chlorine should be larger than 1×10^{-3} atm for the $ZnCl_2$ formation when the oxygen partial pressure was 0.2 atm.

Figure 9 shows the predominance diagrams on the Fe–F–Cl and Fe–Cl–O systems. From Fig. 9(a), FeF_3 is dominant in a relatively high $P_{Cl_2}(=0.1)$. When the partial pressure of fluorine is around 1×10^{-40} atm at 200°C, P_{Cl_2} should be high and around 1×10^{4} atm for the formation of $FeCl_3$, that is, it is almost impossible to form (Fig. 9(c)). These results indicate that Fe_2O_3 and FeF_3 will be dominant in Fe–Cl–F–O system with a relatively high Cl_2 pressure.

4.1. Equilibrium Composition in Zn–Fe–Pb–Mn–Cr–O–Cl–F System

To understand the deposited dust composition, thermodynamic calculation from 1 800°C to ambient temperature was performed. Based on the chemical composition of dust, the rate of vaporization of metallic elements were determined as shown in **Table 1**. Chlorine and fluorine were treated as gas phase at the beginning of the calculation, al-

Table 1. Assumed vaporization rate of elements in dust vaporized and gases in Air. (Data base for thermodynamic calculation)

Dust	Fe	Zn	Pb	Mn	Cr	Cl	F
kmol/min	0.0878	0.0366	0.0021	0.0054	0.0017	0.0134	0.0118
Gas phase	N_2	O_2	Cl_2	F_2			
kmol/min	2.5	0.67	0.0067	0.0059			
%/min	78.55	21.06	0.21	0.18			

Table 2. Elements and compounds taking into account for the equilibrium calculation.

Preliminary Calculation		Final Calculation
Gas Phase	Solid Phase	
$Cl_2(g)$	*C	Gas Phase
*CO(g)	*Cr	$Cl_2(g)$
$CO_2(g)$	Cr_2O_3	$FeF_2(g)$
*Cr(g)	*CrCl	$FeF_3(g)$
*$Cr_2O(g)$	*$CrCl_2$	$MnCl_2(g)$
*$Cr_2O_2(g)$	*CrF	$MnF_2(g)$
*$Cr_2O_3(g)$	*CrF_2	$O_2(g)$
*CrCl(g)	*CrO_2	PbCl(g)
*$CrCl_2(g)$	*CrO_3	$PbCl_2(g)$
*CrF(g)	*Fe	$PbF_2(g)$
*$CrF_2(g)$	Fe_2O_3	PbO(g)
*CrO(g)	Fe_3O_4	Zn(g)
*$CrO_2(g)$	*$FeCl_2$	$ZnCl_2(g)$
*$CrO_3(g)$	*$FeCl_3$	ZnF2(g)
*$F_2(g)$	*FeF_2	ZnO(g)
*Fe(g)	FeF_3	
*FeCl(g)	FeO	
$FeCl_2(g)$	*Mn	
FeF(g)	Mn_2O_3	
$FeF_2(g)$	$MnCl_2$	Solid Phase
$FeF_3(g)$	MnF_2	Cr_2O_3
*FeO(g)	MnF_3	Fe_2O_3
*Mn(g)	MnO	Fe_3O_4
*MnCl(g)	$MnO*Fe_2O_3$	FeF_3
$MnCl_2(g)$	MnO_2	FeO
*MnF(g)	*Pb	Mn_2O_3
$MnF_2(g)$	*Pb_2O_3	$MnCl_2$
*MnO(g)	$PbCl_2$	MnF_2
*$MnO_2(g)$	$PbCrO_4$	MnF_3
$O_2(g)$	PbF_2	MnO
*Pb(g)	*PbO	$MnO \cdot Fe_2O_3$
PbCl(g)	PbO2	MnO2
$PbCl_2(g)$	Zn	$PbCl_2$
*PbF(g)	$ZnCl_2$	$PbCrO_4$
$PbF_2(g)$	$ZnCrO_4$	PbF_2
PbO(g)	ZnF_2	$ZnCl_2$
Zn(g)	$ZnFe_2O_4$	ZnF_2
$ZnCl_2(g)$	ZnO	$ZnFe_2O_4$
*ZnF(g)	$ZnO \cdot Cr_2O_3$	ZnO
$ZnF_2(g)$		ZnO·Cr2O3
ZnO(g)		

*Neglected elements and compounds at final calculation

though those elements originated from solid phase (dust).

Table 2 shows the kinds of compounds which are possible to form from the elements, Zn, Fe, Pb, Mn, Cr, O, Cl and F. In the preliminary calculation, 41 compounds in gas phase and 39 compounds in solid phase were taking into account. An assumed amount of input was shown in Table 1. The SOLGASMIX equilibrium routine which is integrated in the HSC Chemistry package was used to calculate the equilibrium composition. From the result of the preliminary calculation, low concentration compounds less than

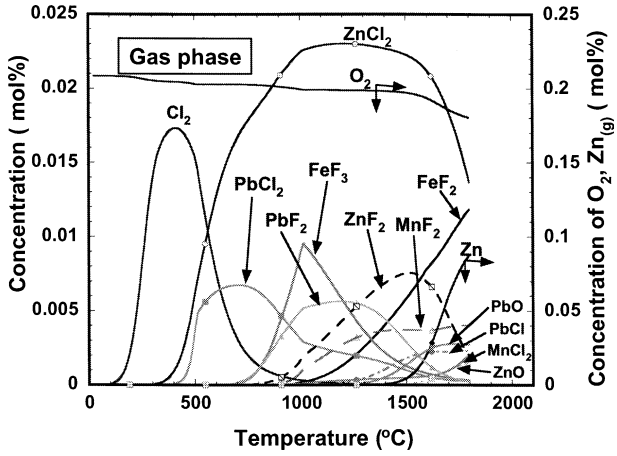

Fig. 10. Variation of equilibrium compounds of gas phase in dust.

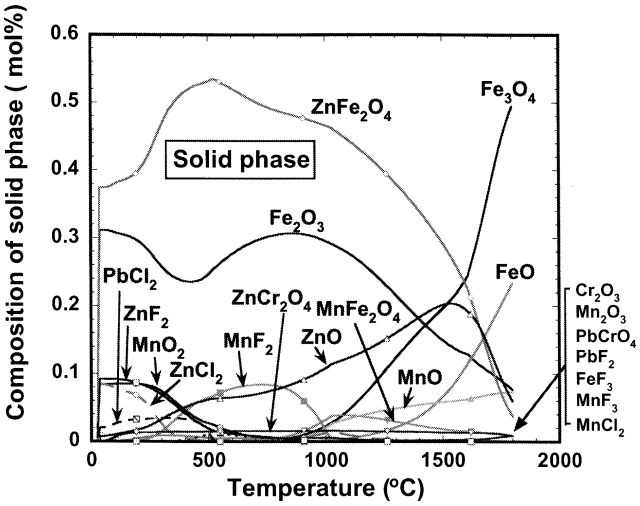

Fig. 11. Variation of equilibrium compounds of solid phase in dust.

0.1 mol%, which were marked by asterisk (*; Table 2), were neglected for the final calculation. 14 compounds in gas phase and 20 compounds in solid phase were taking into account for the final calculation.

Figures 10 and **11** show the calculation results of equilibrium composition in the dust. Figure 10 shows the variation of compounds in gas phase and Fig. 11 shows the one in solid phase.

In higher temperature than 1 400°C, main constituent in gas phase is Zn(g) (except O_2). From 1 400 to 500°C, largest one is $ZnCl_2(g)$, and the second ones are $ZnF_2(g)$, $PbF_2(g)$, $FeF_3(g)$, $PbCl_2(g)$, which are stable in different temperature range (Fig. 10). The maximum chlorine partial pressure exists around 400°C, which means that the injection of humid air for the cooling will increase the HCl content in the gas. This result would be very important to understand the actual dust behavior that the dust sticking occurred inside the filtering system. If all the dust particles were dried, there would be no sticking. The reason of sticking could be explained by the wetting and/or the active surface near the melting point. In these consideration, it might be important the existence of HCl (or Cl_2) and $ZnCl_2$. If the content of HCl gas in the dust increased, the sticking of dust particle would be promoted and the adhesion of dust

inside the blower would increase. How to eliminate the Cl_2 gas evolution and the formation of HCl gas in this temperature range will be the important factor to prevent the dust adhesion in the filtering system. Moreover, as the melting point of $ZnCl_2$ is 287°C, the property of $ZnCl_2$ less than 287°C will be adhesive and it could be a cause of dust adhesion also.

In solid phase (Fig. 11), the main constituents are $ZnFe_2O_4$ and Fe_2O_3. In the temperature range less than 1 000°C, the constituents are ZnO, MnF_2, MnO_2, $ZnCl_2$, ZnF_2 and $PbCl_2$. And the chlorides ZCl_2, $PbCl_2$ and oxides MnO_2 will form less than 500°C. These compounds are in quite good agreement with the result of XRD (Fig. 7). Only MnF_2 and FeF_3 were different between the thermodynamic calculation and the actual dust composition. However, if the fluorides deposited around 1 000°C from gas phase (ref. Fig. 10), the fluorides were FeF_3, PbF_2 and ZnF_2, which were the same compounds in the actual dust. These behaviors of dust deposition were just discussed from the macroscopic point of view by thermodynamic analysis. The microscopic mechanism of dust deposition such as the site of deposition will be very important knowledge. In future, another approach for the dust deposition will be necessary to clarify the microscopic mechanism.

In present study, the existence of oxychloride such as (ZnOCl, FeOCl, *etc.*) did not taking into account.

The behavior of oxychloride will be important for a detailed analysis. Recently, S. H. Son, *et al.* have published the data on the vapor pressure of zinc oxychloride.[19] The formation of gaseous ZnOCl should be considered in high oxygen pressure.

$$ZnCl_2(g)+1/2\,O_2(g)=ZnOCl(g)+1/2\,Cl_2(g) \quad \text{.....(5)}$$

$$\Delta G^\circ=-14.3+0.069T \quad \text{(kJ/mol)} \quad \text{.....(6)}$$

Using Eq. (6), the vapor pressure of ZnOCl is relatively large and almost the same level ($P_{ZnOCl}=0.022$) as Cl_2 gas at 500°C. However, data for other oxychlorides could not be established sufficiently until now. And the ZnOCl gas will deposit as $ZnCl_2$, so that the discussion on the dust deposition will need further experimental data.

5. Conclusions

The dust sampled from the impeller of blower in the dust filtering system of EAF during the dust injection operation was examined by XRD and XRF. Quite complicated compounds formed in Zn–Fe–Pb–Cr–Mn–O–Cl–F system were found in the dust. Thermodynamic analysis from 1 800°C to ambient temperature was performed and the equilibrium composition around ambient temperature obtained from the calculation was in excellent agreement with the actual composition in the dust.

Obtained results are as follows.

(1) Main constituents in the dust are $ZnFe_2O_4$ and Fe_2O_3. Relatively dominant compounds are as follows: Fluorides are FeF_3, ZnF_2 and PbF_2, chlorides are $ZnCl_2$ and $PbCl_2$, and oxides are ZnO and MnO_2.

(2) From the thermodynamic calculation, it was found that the fluorides deposited around 1 000°C from gas phase. And the chlorides ZCl_2, $PbCl_2$ and oxides MnO_2 will form less than 500°C.

(3) The partial pressure of chloride gas becomes a maximum around 400°C, which will form HCl produced by the reaction with moisture in the air. Moreover, deposited $ZnCl_2$ less than the melting point (287°C) will be adhesive. These results will cause to the adhesion of the dust in the filtering system.

REFERENCES

1) S. Hirata, K. Ino and O. Iida: *CAMP-ISIJ*, **14** (2001), 1003.
2) M. Naito, T. Obara and Y. Obara: *CAMP-ISIJ*, **11** (1998), 782.
3) S. Isozaki, T. Hosokawa, T. Maki and N. Sakamoto: *CAMP-ISIJ*, **11** (1998), 159.
4) N. Ishiwata, T. Sato, M. Miyakawa, Y. Hara and H. Itaya: *CAMP-ISIJ*, **10** (1997), 980.
5) M. Kawashima and S. Yokoyama: *CAMP-ISIJ*, **10** (1997), 61.
6) N. Sakamoto, T. Shikada, N. Yamamoto and I. Okouchi: *CAMP-ISIJ*, **10** (1997), 42.
7) K. Inoue: *CAMP-ISIJ*, **10** (1997), 40.
8) T. Hara, H. Sasamoto, Y. Okada and K. Suzuki: *CAMP-ISIJ*, **9** (1996), 802.
9) T. Hara, H. Sasamoto, Y. Okada, K. Suzuki and H. Mizuta: *CAMP-ISIJ*, **10** (1997), 58.
10) A. Tsubone and H. Sasamoto: *CAMP-ISIJ*, **11** (1998), 931.
11) I. Takebayashi, J. Nishi, T. Mizutani, H. Okamura and T. Toyota: *CAMP-ISIJ*, **10** (1997), 46.
12) Y. Enomoto, M. Hattori and T. Okumura: *CAMP-ISIJ*, **6** (1993), 1103.
13) H. Sasamoto, J. P. Birat and M. Faral: *CAMP-ISIJ*, **13** (2000), 790.
14) T. Momiyama, M. Furutera, K. Hayashida, H. Sasamoto and A. Tsubone: *CAMP-ISIJ*, **16** (2003), 183.
15) K. Igarashi, T. Nakamura, S. Kimura and K. Iwata: *CAMP-ISIJ*, **15** (2002), 735.
16) H. W. Gudenau, K. Stoesser, H. Denecke and V. Schemmann: *ISIJ Int.*, **40** (2000), 218.
17) H. Sasamoto: *CAMP-ISIJ*, **10** (1997), 2.
18) A. Nakamura and T. Yoshida: *CAMP-ISIJ*, **10** (1997), 6.
19) S. H. Son and F. Tsukihashi: *ISIJ Int.*, **43** (2003), 1356.